ISSN: 0067-2904

Estimation of the Efficiency of Corrosion Inhibition by Zn-Dithiocarbamate Complexes: a Theoretical Study

Mustafa M. Kadhim[1], Layla A. Al. Juber[2], Ahmed S. M. Al-Janabi [3, *]
[1] Department of Chemistry, College of Science, Wasit University, Kut, Wasit, Iraq
[2]Department of Chemistry, College of Science, Tikrit University, Tikrit, Iraq
[3]Department of Biochemistry, College of Veterinary Medicine, Tikrit University, Tikrit, Iraq

Received: 17/9/2020 Accepted: 31/3/2021

Abstract
Seven Zn-dithiocarbamate complexes were suggested as corrosion inhibitors. Density functional theory (DFT) was used to predict the ability of inhibition. Room temperature conditions were applied to suggest the optimization of complexes, physical properties, and corrosion parameters. In addition, the HOMO, LUMO, dipole moment, energy gap, and other parameters were used to compare the inhibitors efficiency. Gaussian 09 software with LanL2DZ basis set was used. Total electron density (TED) and electrostatic surface potential (ESP) were utilized to show the sites of adsorption according to electron density.

Keywords: DFT, Corrosion inhibition, Zinc compounds, HOMO, LanL2DZ

تقدير تثبيط التآكل لمعقدات الزنك- ثنائي ثايوكاربراميت " دراسة نظرية"

مصطفى محمد كاظم [1] ، ليلى عبدالرحمن ال-جبر[2] ، احمد شاكر الجنابي[3*]
[1] قسم الكيمياء، كلية العلوم، جامعة واسط ، الكوت ، واسط ، العراق
[2] قسم الكيمياء، كلية العلوم، جامعة تكريت ، تكريت ، العراق
[3] فرع الكيمياء الحياتية، كلية الطب البيطري، جامعة تكريت ، تكريت ، العراق

الخلاصة
تم اقتراح سبعة معقدات Zn-dithiocarbamate كمثبطات للتآكل. استخدمت نظرية الكثافة الوظيفية (DFT) للتنبؤ بقدرة التثبيط. أجريت الدراسة في درجة حرارة الغرفة لاقتراح تحسين المعقدات والخواص الفيزيائية ومعاملات التآكل. بالإضافة إلى ذلك، HOMO و LUMO والعزم ثنائي القطب وفجوة الطاقة والمزيد من العوامل المستخدمة لمقارنة كفاءة المثبطات. تم استخدام برنامج Gaussian 09 مع مجموعة أساسية LanL2DZ. واستخدمت كثافة الإلكترون الكلية (TED) وجهد السطح الكهروستاتيكي (ESP) لإظهار مواقع الامتزاز وفقًا لكثافة الإلكترون.

Introduction

Metal complexes of dithiocarbamate compounds have been the substance of a recently growing interest because it possesses a wide range of applications in agricultural science, medicine, industry, and analytical and organic chemistry [**1-10**]

* Email: dr.ahmed.chem@tu.edu.iq

The corrosion of metal is considered as the most serious problem in the field of industry [**11**]. Researchers have developed a considerable expertise in developing optimal protection for metals [**12**]. Many methods are being applied to prevent the corrosion process, one of them is the usage of inhibitors. The chemical compounds are a common use in this line. The most favorable types of compounds is those that contain polar atoms, such as oxygen, sulfur, phosphorus, nitrogen etc., which include a single pair of electrons that can be attracted to the metal surface by the adsorption process, forming a protective layer [**13**]. Dithiocarbamate is a ligand that can act as a corrosion inhibitor due to the presence of sulfur and nitrogen as electronegative atoms [**14**]. Recently, many studies were published that involve the utilization of metal-dithiocarbamate compounds (such as Zn(II) N-Isopropylbenzyldithiocarbamate) as corrosion inhibitors [**15-17**]. In addition, theoretical studies have been applied in this line to save time, money, and effort to suggest the best inhibitor [**18**]. Many researchers used dithiocarbamate compounds as corrosion inhibitors, such as sodium N,N-diethyldithiocarbamate, ammonium pyrrolidine dithiocarbamate, ammonium (2,4-dimethylphenyl)-dithiocarbamate, azepane dithiocarbamate, and others [**19-32**]. In this study, a theoretical study for the inhibition of corrosion by zinc compounds is conducted.

Preparation of compounds

The Zn-dithiocarbamate compounds used in this study were prepared by previously described methods [**3, 33**].

Calculation Methods

The quantum chemical calculations were performed by Gaussian-09 software package with complete geometry optimizations [**34, 35**] that applied for the inhibitors which shown in **(Figure- 1)** by using the density functional method (DFT, B3LYP/LanL2DZ) [**36**]. All calculations are achieved in the vacuum medium [**37, 38**]**.** The results of the Gaussian analysis are demonstrated in the Supplementary Information (Figure- S1).

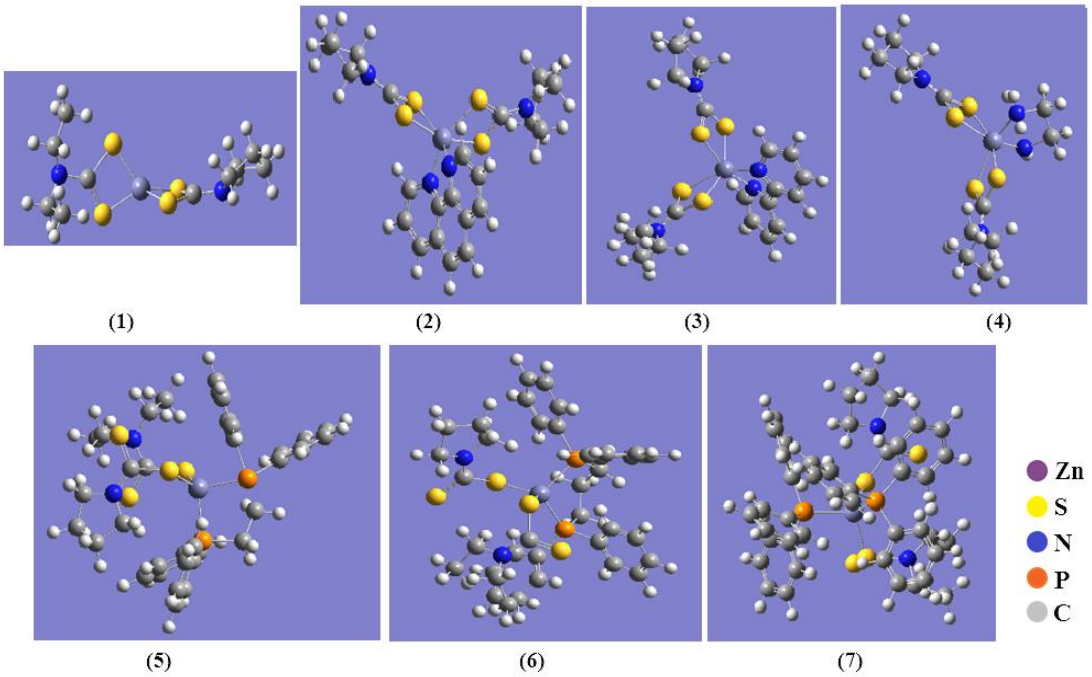

Figure 1- Two dimensional structures of the Zn-dithiocarbamate complexes (**1-7**)

Results and Discussion

Inhibition Parameters

The prediction of absorbed inhibitor molecules was achieved by applying the limits orbital theory in respect to attraction the centers of these molecules to the metal surface [**39**]. This process involves the fragment molecular orbital (FMO) of the border, which gives the contribution through the inverse of the energy requirement of the stability of the difference in orbital energy ($\Delta E = E_{LUMO}-E_{HOMO}$). The

ability to donate an electron to an acceptor can be expressed by the energy HOMO (EHOMO). The high values of EHOMO for the inhibitor molecule give it a tendency to donate electrons. While the ability of the molecule to accept an electron is referred to as the energy LUMO (ELUMO), the lowest value of which means a higher electron accepting capacity. The energy gap between the orbits of the border (ΔE) is important in the explanation of the compound's activity; when the energy gap is decreased, the effectiveness of the inhibitor is improved [**39**]. The quantum chemical parameters are related to the efficiency of the inhibition of the molecule studied. These parameters include the highest molecular orbital energy (E_{HOMO}) occupied by electrons, the lowest unoccupied molecular orbital energy (E_{LUMO}), the energy gap ($\Delta E= E_{LUMO}-E_{HOMO}$), the dipole moment (μ), electronegativity (χ),the effort ionization (IP), electron affinity (EA), and the global softness (S), as shown in Tables- 1 and 2.

According to the theory of Koopman [**39**], HOMO energy is related to the ionization potential (IE) whereas LUMO energy is linked to the electron affinity (EA), as follows:

$IE = -E_{HOMO}$ …..(1)

IE is the amount of energy required for removing an electron from an atom. The low ionization energy gives high efficiency for inhibition.

$EA = -E_{LUMO}$ …..(2)

EA is the quantity of energy released when an electron is added to an atom. The higher values of EA means less stability and produces high efficiency for inhibition.

Hardness (η) is the second derivative of E, which measures both the stability and reactivity of the compound [**40**].

$$\eta = \frac{IE-EA}{2} \quad ....(3)$$

$$X = -\mu = \frac{IE+EA}{2} \quad .....(4)$$

This value is related to HOMO and LUMO energies. The low value of electronegativity means high efficiency for inhibition.

The global softness (S) is the inverse of the global hardness [**41**]. Softness is one of the important properties to measure the compound's stability and reactivity:

$$S = \frac{1}{\eta} \quad .....(5)$$

Global electrophilicity index (ω) was discussed by Parr [**42**]. It is a measure of the stabilization in energy after a compound accepts an added number of electrons. A good inhibitor should have a lower (ω) value.

$$\omega = \frac{(-X)^2}{2\eta} \quad ….(6)$$

ΔE	4>7>3>2>6>5>1
μ	7>6>5>4>1>2>3
HOMO	4>7>3>2>6>5>1
LUMO	6>5>7>1>4>2>3
IA	4>7>3>2>6>5>1
EA	6>5>7>1>4>2>3
χ	3>4>7>2>6>5>1
η	4>7>3>2>6>5>1
S	4>7>3>2>6>5>1
ω	3 > 4 > 2 > 7 >5>6>1

According to the parameters (such as HOMO, ΔE , IA, and η), the final order of the complexes is:
4 > 7 > 3 > 2 > 6 > 5 > 1

The energy gap is proportional to the final order of complexes, and it is represents the most important factor.

Table 1-DFT values calculated for E_{HOMO}, E_{LUMO}, $\Delta E_{HOMO-LUMO}$ and μ of the inhibitor compounds investigated in the present study.

Inhibitor	E_{HOMO} (eV)	E_{LUMO} (eV)	$\Delta E_{HOMO-LUMO}$ (eV)	μ (Debye)
1	-5.9411	0.1997	6.1409	2.7506
2	-3.0643	0.6296	3.6940	2.6889
3	-2.7696	0.8596	3.6292	1.6705
4	-2.3532	0.3072	2.6605	7.0989
5	-4.2951	0.1063	4.4015	7.6096
6	-4.1468	0.0419	4.1887	9.2372
7	-2.5364	0.1763	2.7127	15.3546

Table 2-Quantum chemical parameters for the inhibitor molecules in vacuum medium as calculated using DFT method.

Inhibitor	IE (eV)	EA (eV)	χ(eV)	η (eV)	S (eV)	ω (eV)
1	5.9411	-0.19974	2.8707	3.0704	0.3256	1.3419
2	3.0643	-0.6296	1.2173	1.8470	0.5414	0.4011
3	2.7696	-0.8596	0.9550	1.8146	0.5510	0.2513
4	2.3532	-0.3072	1.0230	1.3302	0.7517	0.3933
5	4.2951	-0.1064	2.0943	2.2007	0.4543	0.9965
6	4.1468	-0.0419	2.0524	2.0943	0.4774	1.0056
7	2.5364	-0.1763	1.1800	1.3563	0.7372	0.5133

HOMO-LUMO Molecular Orbital

Figure-2 illustrates that the inhibitor compounds 4, 7 and 3 showed best inhibitory effects, based on the geometries optimization of compounds studied in the gas phase, including LUMO and HOMO density distributions. The supplementary Figure- S4 includes results of the other inhibitors. The red color indicates high electron density while the green represents low electron density [**43**]. High electron density area is the donating area of electrons to the metal. Low electron density area is the receiving area of electrons from the metal [47]. Hence, the two areas have very important distribution.

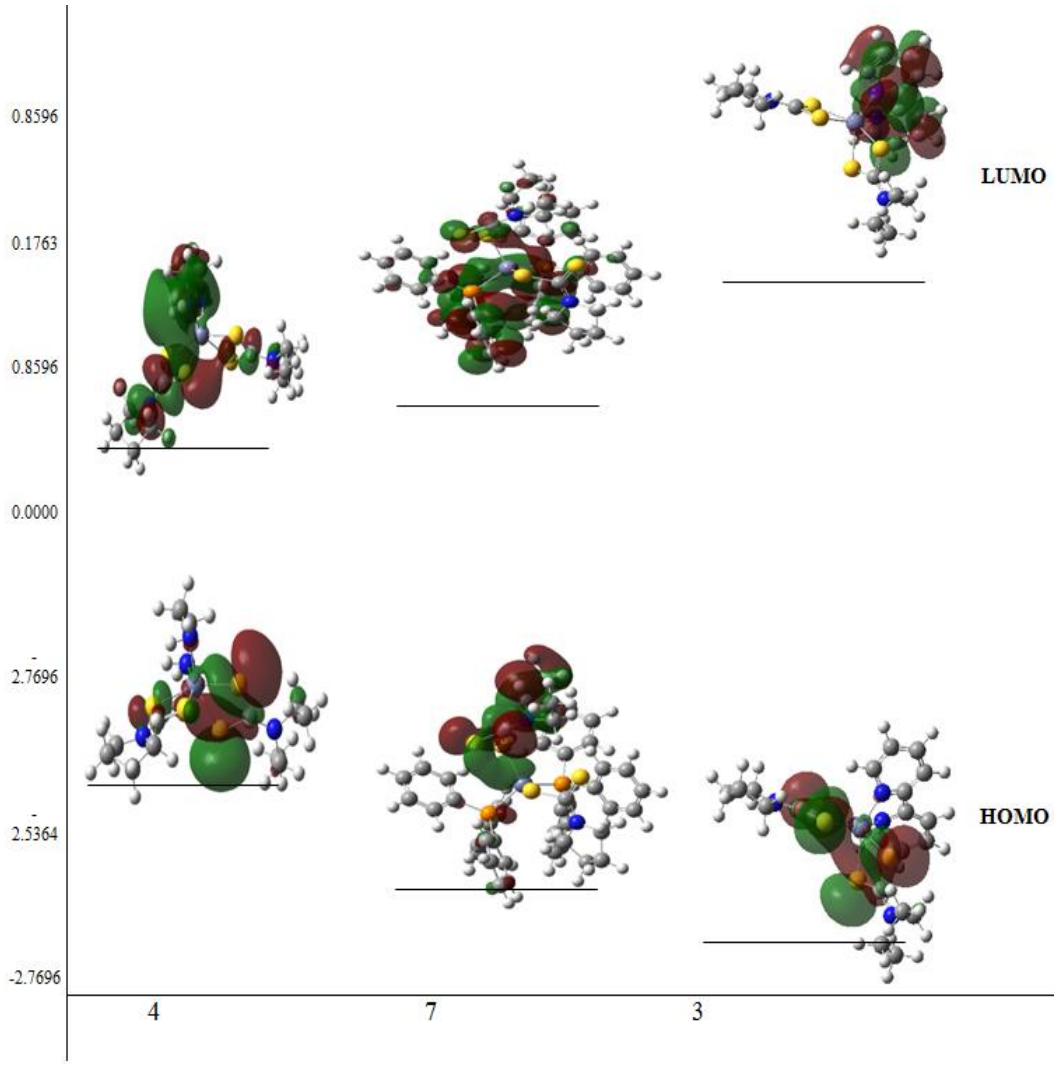

Figure 2- The energy level (HOMO-LUMO) orbitals of the best-studied inhibitors (**4, 7** and **3**).

TED and ESP Maps

TED map presented the electron density on the complexes. The red color is due to the sites with high electron negativity; for example, the S atom and some areas of double bond in the studied molecules, which can help in the electrophilic attack. Whereas the yellow color refers to the atoms with moderate electronegativity. The blue color is assigned to the best positive area that can accept electrons from the donor compound [**44**], as in **(Figure-3).** The electrostatic surface potential (ESP) shows the adsorption direction of the complex with the metal surface, which is the same direction of the aromatic rings, S and N atoms. The green surface can be considered as the surface of the metal or alloy. **Figure- 4** shows the ESP values of the inhibitors (**1-7**).

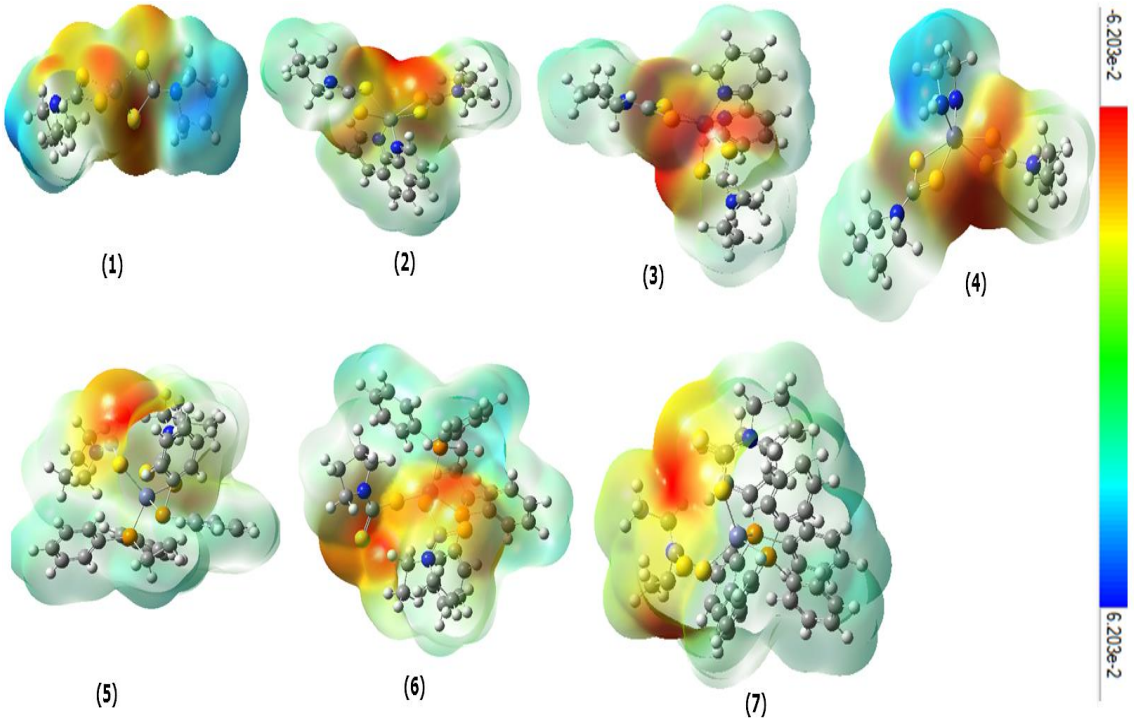

Figure 3- TED maps of the inhibitors.

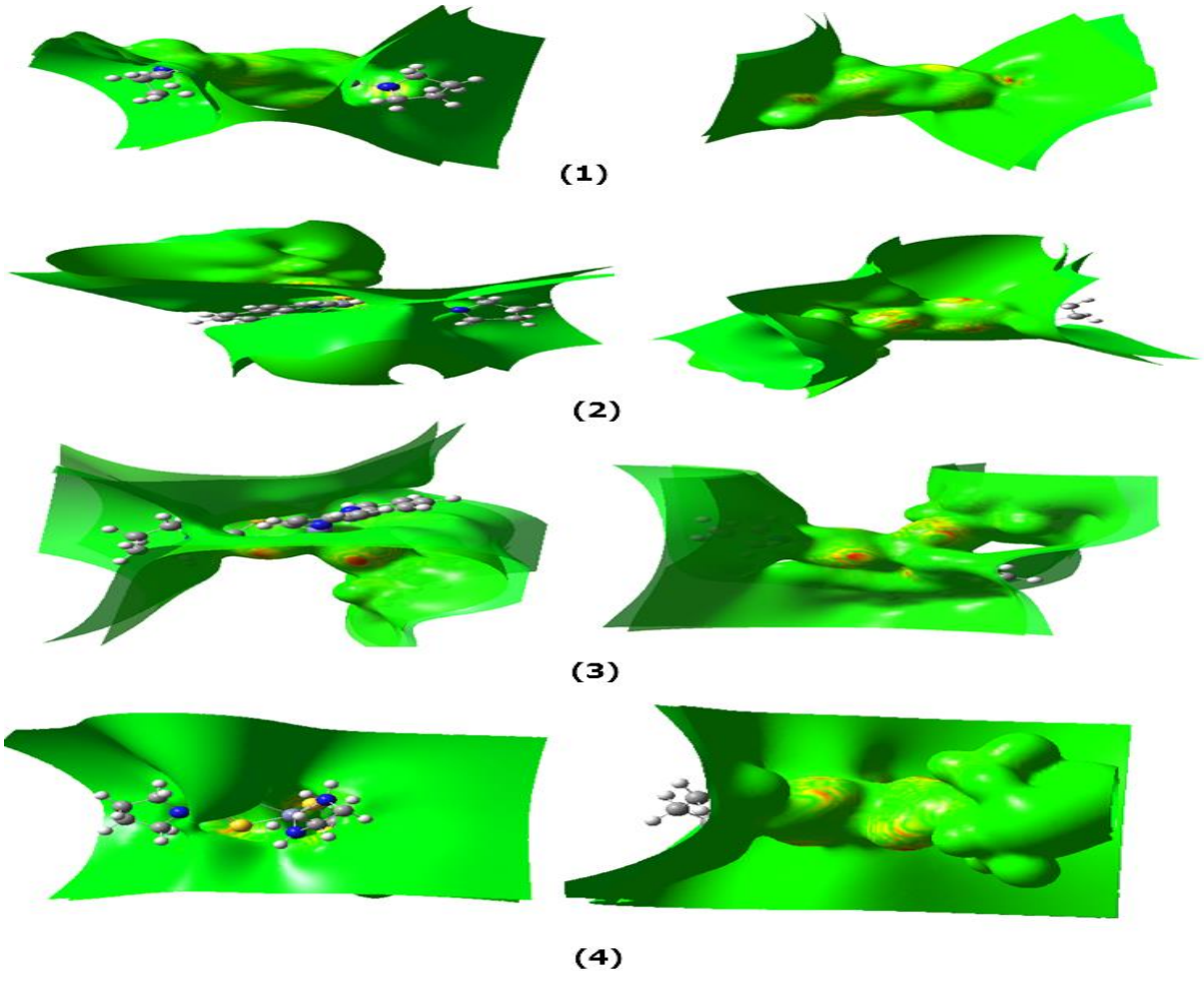

Figure 4- ESP maps of the inhibitors (**1-4**).

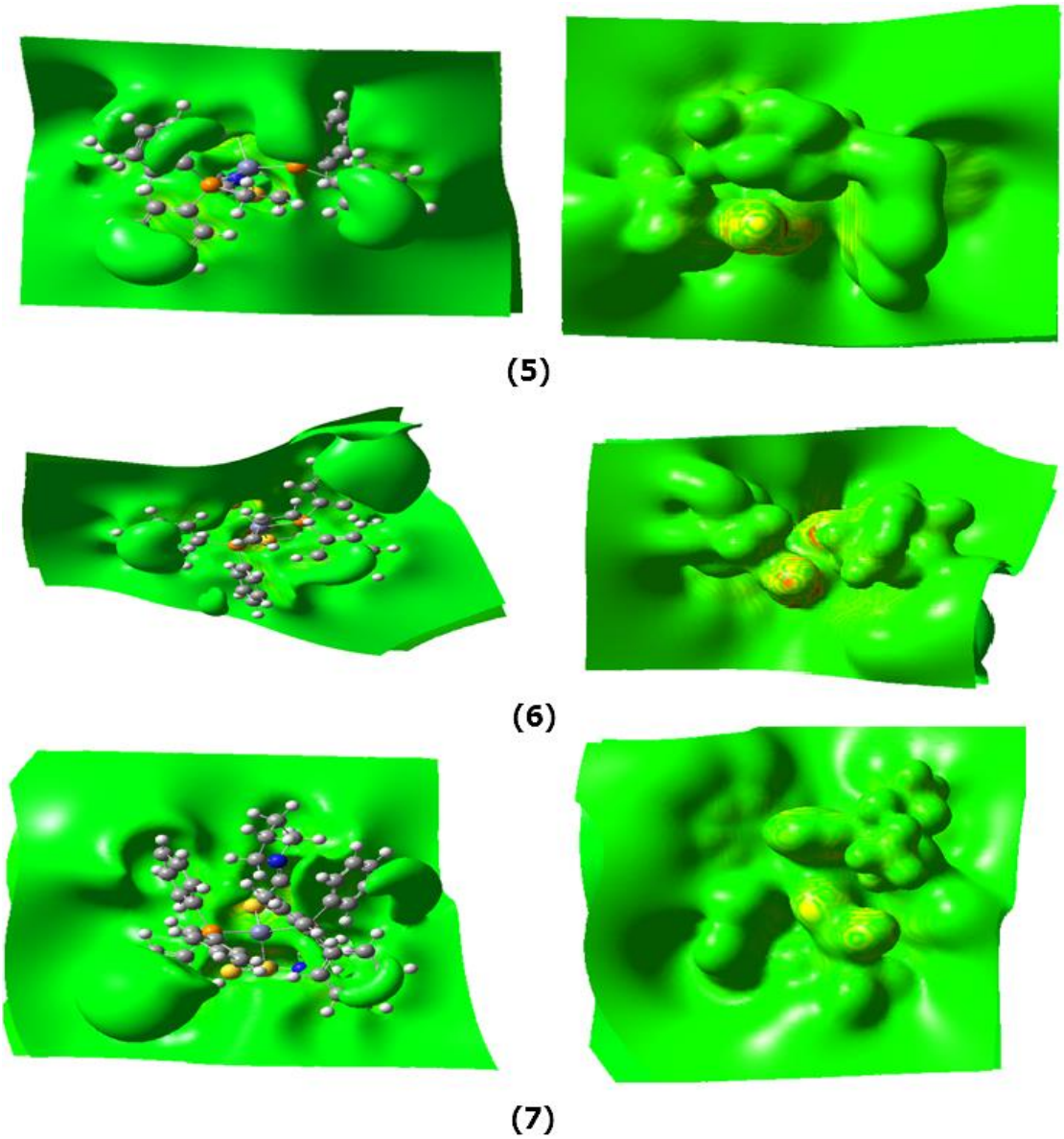

Figure 4-(continued) - ESP maps of the inhibitors (**5-7**).

Conclusions

The present study showed the ability of corrosion inhibition by seven compounds. According to the parameters applied, the most efficient inhibiters were 4, 7 and 3, respectively. The aromatic rings, N and S, in the compounds were allowed to donate and accept electrons with the metal. The most effective parameters were the dipole moment and energy gap, which showed values of 7.0989, 15.3546 and 1.6705 Debye and 2.6605, 2.7127 and 3.6292 eV for the inhibitors 4, 7 and 3, respectively. The compounds 1, 2, 5 and 6 had lower inhibition abilities than those of the compounds 4, 7 and 3.

References

1. Hogarth, G. **2012,** Metal-dithiocarbamate complexes: chemistry and biological activity, *Mini-Reviews in Medicinal Chemistry*., **12**: 1202–1215. https://doi.org/10.2174/138955712802762095 .
2. Odularu A.T., Ajibade P.A. **2019**. Dithiocarbamates: Challenges, control, and approaches to excellent yield, characterization, and their biological applications, *Bioinorganic Chemistry and Applications*. 2019, pp: 878-892. https://doi.org/10.1155/2019/8260496.

3. Al-Janabi A. S. M. , Saleh A. M., Hatshan M. R. **2021**. Cytotoxicity, antimicrobial studies of M(II)-dithiocarbamate complexes, and molecular docking study against SARS COV2 RNA-dependent RNA polymerase. *Journal of Chines Chemical Society*. pp:1–12. https://doi.org /10.1002 /jccs.202000504.

4. Al-Jibori S. A., Al-Janabi A. S. M. , Al-Sahan S.W.M., Wagner C. **2021**. Pd (II)- pyrrolidine dithiocarbamate complexes: Synthesis, spectroscopic studies and molecular structure of [Pd(PyDT)(ppy)], *Journal of Molecular Structure*, **1227**: 129524, https://doi.org/10.1016/j.molstruc.2020.129524.

5. Al-Janabi, A.S.M., Kadhim, M.M., Al-Nassiry, A.I.A., Yousef, T.A. **2021**. Antimicrobial, computational, and molecular docking studies of Zn (II) and Pd (II) complexes derived from piperidine dithiocarbamate, *Applied Organometallic Chemistry*, **35**(2): e6108. https://doi.org /10.1002/aoc.6108

6. Hogarth G., **2005,** Transition metal dithiocarbamates: 1978-2003, *Progress in Inorganic Chemistry*, Edited by Kenneth D. Karlin,, 53: 71-585, https://doi.org/10.1002/0471725587.ch2 .

7. Kanchi, S. Singh P., Bisetty K., **2014**. Dithiocarbamates as hazardous remediation agent: A critical review on progress in environmental chemistry for inorganic species studies of 20th century, *Arabian Journal of Chemistry*. **7**: 11–25. https://doi.org/10.1016/j.arabjc.2013.04.026 .

8. Al-Nassiry A. I. A., Al-Janabi, A. S. M., Al-Janabi , O. Y. T. Spearman, P. Al-Heety, M. A. **2020**, Novel dithiocarbamate – Hg (II) complexes containing mixed ligands : Synthesis , spectroscopic characterization , and H 2 storage capacity, *Journal of Chines Chemical Society*. **67**: 775–781.https://doi.org/10.1002/jccs.201900349.

9. Al-Janabi, A. S. M., Al-Samrai, O. A. Y., Yousef T. A. **2020**. New palladium(II) complexes with 1-phenyl-1H-tetrazole-5-thiol and diphosphine Synthesis, characterization, biological, theoretical calculations and molecular docking studies, *Applied Organometallic Chemistry*, Accept, e5967,https://doi.org/10.1002/aoc.5967

10. Salman, M. M. Al-Dulaimi, A. A. Al-Janabi, A. S. M. Al-Heety, M. A. **2020**. Novel dithiocabamate nano Zn(II), Cd(II) and Hg(II) complexes with pyrrolidine dithiocarbamate and N,N-diethyldithiocarbamate, *Materials Today: Proceedings*, Accept. https://doi.org/10.1016/j.matpr.2020.07.082

11. Ali G. Q., Tomi I. H. R. **2018**. Synthesis and characterization of new mesogenic esters derived from 1,2,4-oxadiazole and study the effect of alkoxy chain length in their liquid crystalline properties. *Liquid Crystal*, **231**: 234-246

12. Ammal P. R., Prasad R., John S., Joseph A. **2019**, Protection of mild steel in hydrochloric acid using methyl benzimidazole substituted 1, 3, 4-oxadiazole: computational, electroanalytical, thermodynamic and kinetic studies. *Journal Adhesives Science Technology* , **45**: 178-192.

13. Ammar I. A., El Khorafi F. M. **1973**. Adsorbability of thiourea on iron cathodes. *Material Corrosion*, **24**(8): 702–707.

14. Hong-bo, F., Hui-long, W., Xing-peng, G. and Jia-shen, Z. **2002**. Corrosion inhibition mechanism of carbon steel by sodium N,N-diethyl dithiocarbamate in hydrochloric acid solution, *Anti-Corrosion Methods and Materials*, **49** (4): 270-276.

15. Noor S. H. L., Sheikh A. I. S. M. G., Erna N. A., Azizul Hakim L., Mohammad F. N., and Nur N. D. **2018**. Synthesis, Structural, Density Functional Theory, and X-Ray Diffraction Study of Zn(II) N-Isopropylbenzyldithiocarbamate: Anti-Corrosion Screening in Acid Media, *Indonesian Journal of Chemistry*, **18** (4): 755 – 765

16. Mirzakhanzadeh, Z., Kosari, A., Moayed, M.H., Naderi, R., Taheri, P., and Mol, J.M.C. **2018**. Enhanced corrosion protection of mild steel by the synergetic effect of zinc aluminum polyphosphate and 2-mercaptobenzimidazole inhibitors incorporated in epoxy-polyamide coatings, *Corrosion Sci*ence, **138**: 372–379.

17. Iman M., Taghi S., Mohammad M. and Mazdak I. **2020**. Cerium/diethyl dithiocarbamate complex as a novel corrosion inhibitive pigment for AA2024-T3, *Science Reprots*, **10**: 5043-5053

18. Ahmed H. Radhi, Ennas AB. Du, Fatma A. Khazaal, Zaid M. Abbas, Oday H. Aljelawi, Salam D. H., Haider A. A. and Kadhim M. M. **2020**. HOMO-LUMO Energies and Geometrical Structures Effecton Corrosion Inhibition for Organic Compounds Predict by DFT and PM3 Methods, *NeuroQuantology*, **18** (1): 37-45.

19. Iman M., Taghi S., Mohammad M., Mazdak I. **2020**. Cerium/diethyldithiocarbamate complex as a novel corrosion inhibitive pigment for AA2024-T, *Science reports*, 10: 5043-5052.
20. Nur K., Tansug G. ,Mehmet E., Tunç T. **2016**. Investigation of ammonium (2,4-dimethylphenyl)-dithiocarbamate as a new, effective corrosion inhibitor for mild steel, *Corrosion Science*, **105**: 305-313
21. Kanchi S., Singh P., Bisetty K., **2014**. Dithiocarbamates as hazardous remediation agent: a critical review on progress in environmental chemistry for inorganic species studies of 20th century. *Arabian Journal Chemistry*, **7**: 11-25.
22. Ponnuchamy P. Kong M. L., Kuppanagounder P. E. **2013**. Synthesis, spectral characterization, crystal structures and catalytic activity of a series of lanthanide(III) azepane dithiocarbamate complexes, *Polyhedron* , **54**(12): 60–66
23. Qu, L. Li, Bai Q. W., Yang F., Chen Y., Zhang S., Ding Z. **2012**. Sodium diethyldithiocarbamate as a corrosion inhibitor of cold rolled steel in 0.5 M hydrochloric acid solution, *Corrosion Science*, **59**: 249-257.
24. Liao Q.Q., Yue Z.W., Yang D., Wang Z.H., Li Z.H., Ge H.H., Li Y.J. **2011**. Self-assembled monolayer of ammonium pyrrolidine dithiocarbamate on copper detected using electrochemical methods, surface enhanced Raman scattering and quantum chemistry calculations, *Thin Solid Film* , **519**: 6492-6498.
25. Liao Q.Q., Yue Z.W., Yang D., Wang Z.H., Li Z.H., Ge H.H., Li Y.J. **2011**. Inhibition of copper corrosion in sodium chloride solution by the self-assembled monolayer of sodium diethyldithiocarbamate, *Corrosion Science*, **53**: 1999-2005.
26. Fan H.-B. Wang H.-L. Guo Xing-peng, Zheng J. **2002**. Corrosion inhibition mechanism of carbon steel by sodium N,N-diethyl dithiocarbamate in hydrochloric acid solution, *Anti-Corrosion Methods and Materials*, **49**(4): 270-276
27. Mahmoud A. Morad, A. M. K. El-Dean. **2006**. 2,2′-Dithiobis(3-cyano-4,6-dimethylpyridine): A new class of acid corrosion inhibitors for mild steel, *Corrosion Science*, **48**(11): 3398-3412
28. Fan H.B., Fu C.Y., Wang H.L., Guo X.P., Zheng J.S. **2002**. Inhibition of corrosion of mild steel by sodium n,n-diethyl dithiocarbamate in hydrochloric acid solution, *British Corrosion Journal*. **37**: 122-125.
29. Liu W, Duan H, Wei D, Cui B, Wang X. **2019**. Stability of diethyl dithiocarbamate chelates with Cu (II), Zn (II) and Mn (II), *Journal of Molecular Structure*. **1184**: 375–381.
30. Eva A. Yaqo, Rana A. Anaee, Majid H. Abdulmajeed, Ivan H. R. Tomi and Mustafa M. Kadhim. **2020**. Potentiodynamic polarization, surface analyses and computational studies of a 1,3,4-thiadiazole compound as a corrosion inhibitor for Iraqi kerosene tanks, *Journal of Molecular Structure*, **1202**: 127356.
31. Eva A. Y., Rana A. A., Majid H. A., Ivan H. R. and Mustafa M. K. **2019.** Electrochemical, morphological and theoretical studies of an oxadiazole derivative as an anti-corrosive agent for kerosene reservoirs in Iraqi refineries, *Chemical Papers*, **4**: 9883-9892.
32. Eva A. Y., Rana A. A., Majid H. A., Ivan H. R. and Mustafa M. K. **2020** Comparative Study of Different Organic Molecules as an Anti-Corrosion for Mild Steel in Kerosene, *Engineering and Technology Journal*, **38**: 423-430.
33. Amenah I. A. Al-Nassiry, and Ahmed S. M. Al-Janabi, **2020**, Synthesis and characterization of Zn(II) complexes with pyrrolidine and N,N-diethyl-dithiocarbamate and diphosphine or amine ligands , *Tikrit Journal for Pure Science.* 26(4): 78-85.
34. Frisch, M.J. Trucks, G.W. Schlegel, H.B. **2009**, GAUSSIAN 09, Revision D.01 Gaussian, Inc., Wallingford, CT,.
35. Frank J. D., Duminda S. R., Kyle T., and George A. P., **2013**, Evaluation of the Heats of Formation of Corannulene and C60 by Means of Inexpensive Theoretical Procedures *Physical Chemistry Research A.* 117, 4726–4730.
36. Abbas W. S., Ghani U. R., Norbani A., Srinivasa B., Salasiah E. , Hassan H. A. **2015**, Synthesis, characterization, density function theory and catalytic performances of palladium(II)–N-heterocyclic carbene complexes derived from benzimidazol-2-ylidenes. *Inorganica Chimica Acta*, **438**: 14–22.
37. Kubba RM, Khathem MM. **2016**, Theoretical studies of corrosion inhibition efficiency of two new N-phenyl-ethylidene-5- bromo isatin derivatives. *Iraqi Journal of Science*. **57**(2B):1041-1051.

38. Issa, R.M., Awad, M.K. and Atlam, F.M., **2008**. Quantum chemical studies on the inhibition of corrosion of copper surface by substituted uracils. *Applied Surface Science*, **255**(5): 2433–2441.
39. Koopmans, T. **1933**. Über die zuordnung von wellen funktionen und eigenwerten zu den einzelnen elektronen eines toms. *Physica*., **1**: 104-113.
40. Rauk, A. **2001**, "*Orbital Interaction Theory of Organic Chemistry*". 2nd Edition. John Wiley &Sons, New York.
41. Pearson, R.G. **1988**. Absolute electronegativity and hardness application to inorganic chemistry. *Inorganic Chemistry*, **27**(4): 734-740.
42. Parr, R.G. and Pearson, R.G. **1983**. Absolute hardness: companion parameter to absolute electronegativity. *Journal of American Chemical Society.*, **105**: 7512-7516.
43. Kubba RM, Khathem MM. **2016**, Theoretical studies of corrosion inhibition efficiency of two new N-phenyl-ethylidene-5- bromo isatin derivatives. *Iraqi Journal of Science*. **57**(2B):1041-1051.
44. Ennas Abdul Hussein, Ihsan Mahdi Shaheed, Raghad Saad Hatam, Mustafa M. Kadhim, Dhuha Talib Al-Kadhum, Elaf Abd AL-kareem, **2020**, Adsorption, Thermodynamic and DFT Studies of Removal RS Dye on the Iraq Clay from Aqueous Solutions", Sys Rev Pharm ; **11**(3): 495

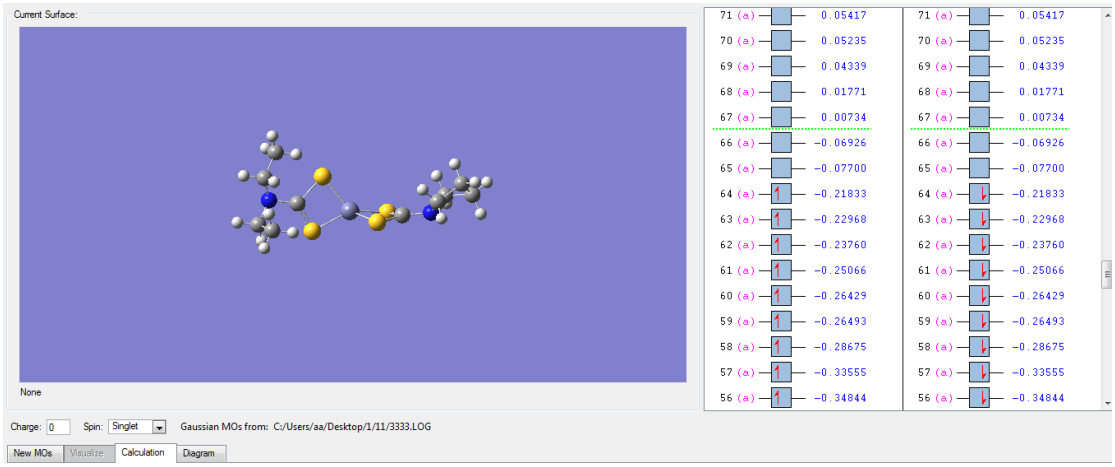

1

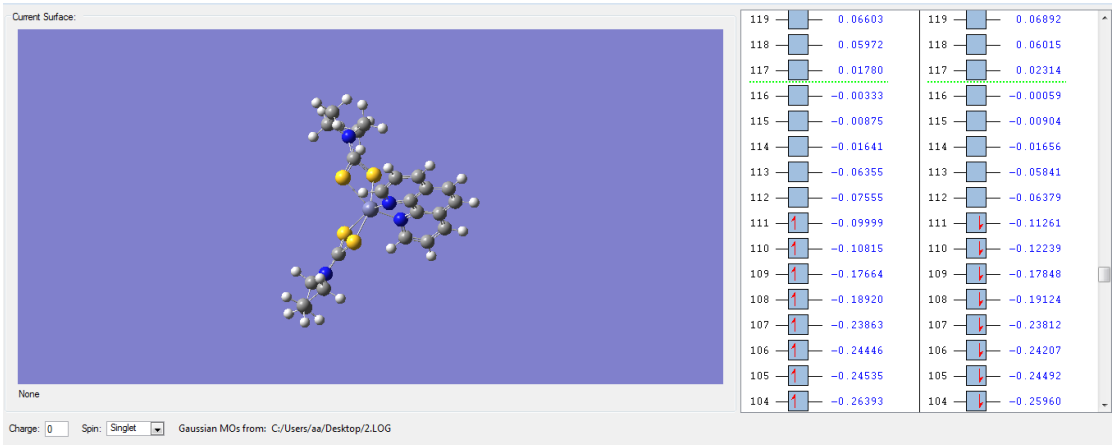

2

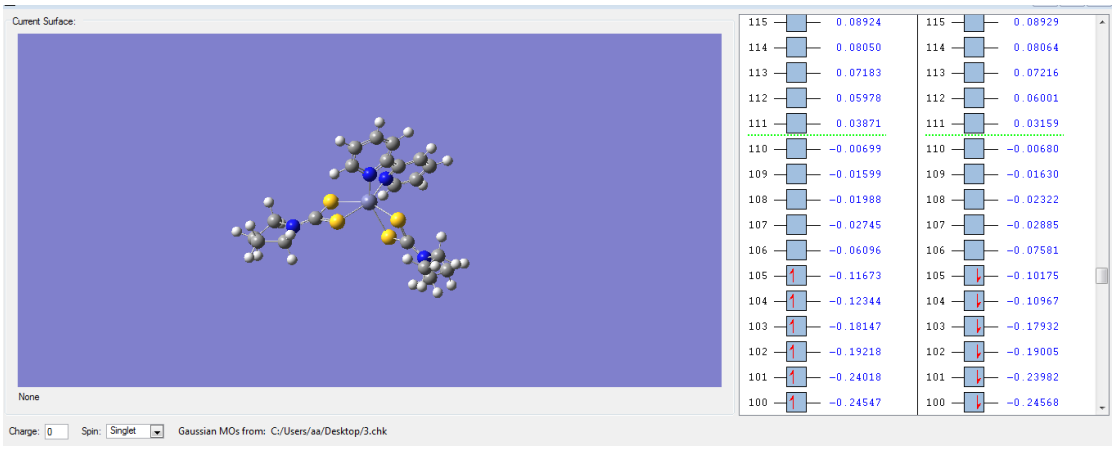
Current Surface:
None
Charge: 0
Spin: Singlet
Gaussian MOs from: C:/Users/aa/Desktop/3.chk

3

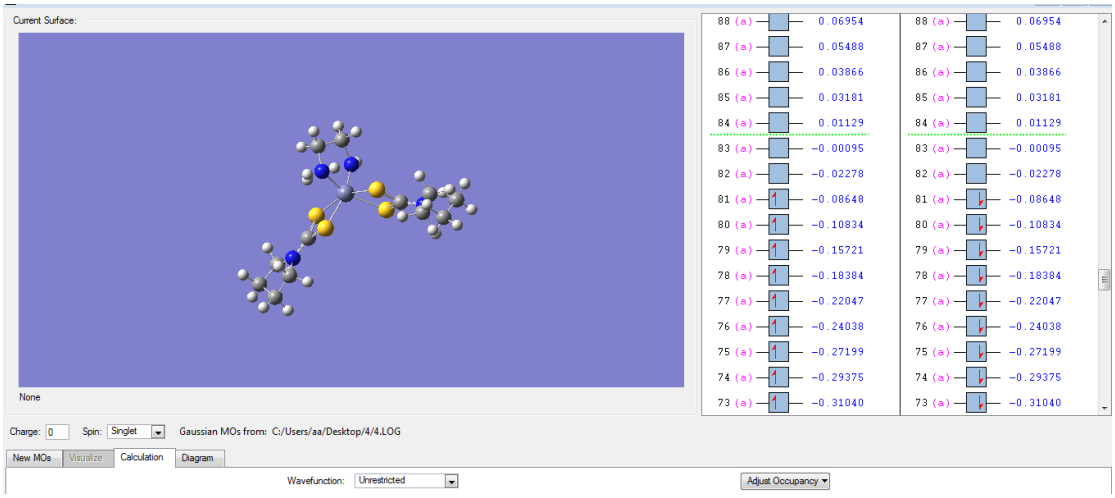
Current Surface:
None
Charge: 0
Spin: Singlet
Gaussian MOs from: C:/Users/aa/Desktop/4/4.LOG
New MOs
Visualize
Calculation
Diagram
Wavefunction: Unrestricted
Adjust Occupancy

4

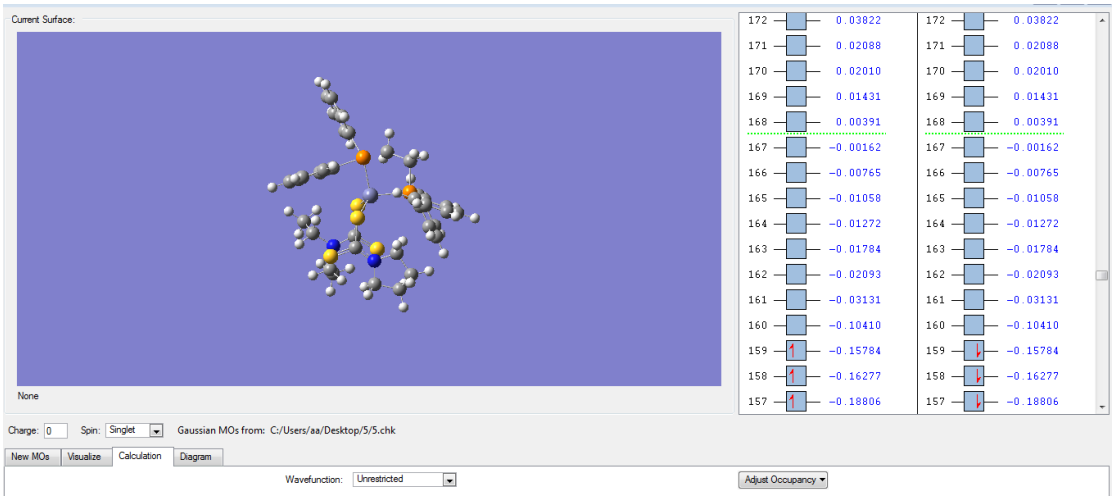
Current Surface:
None
Charge: 0
Spin: Singlet
Gaussian MOs from: C:/Users/aa/Desktop/5/5.chk
New MOs
Visualize
Calculation
Diagram
Wavefunction: Unrestricted
Adjust Occupancy

5

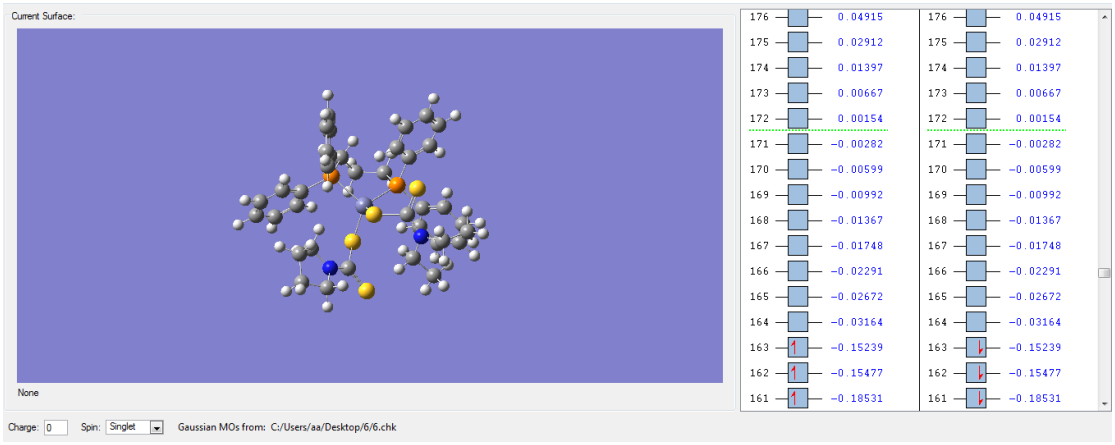

6

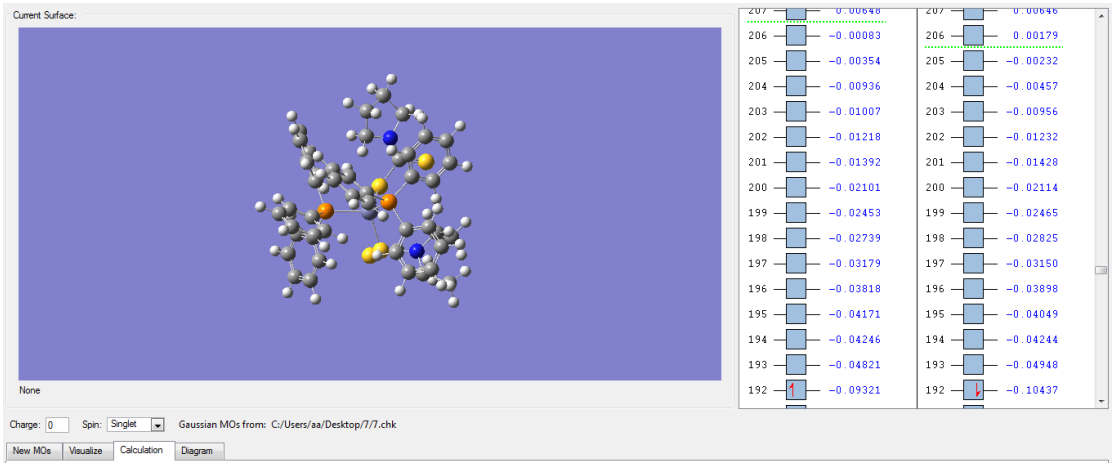

7

Figure 1- Gaussian results in atomic units of 1, 2, 3, 4, 5, 6 and 7 compounds.

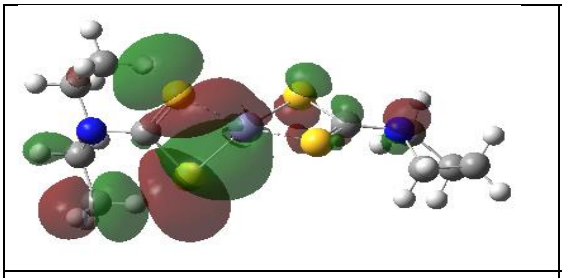

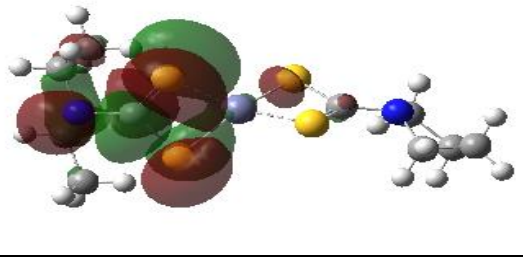

HOMO	LUMO
1	

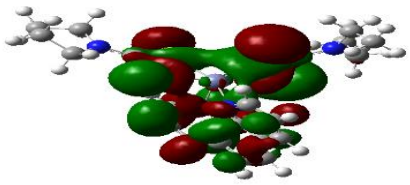

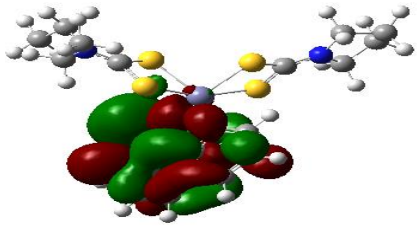

HOMO	LUMO
2	

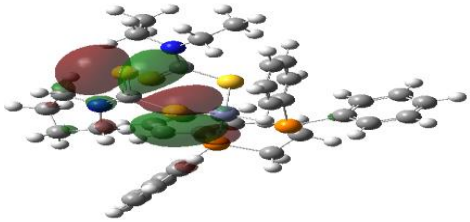	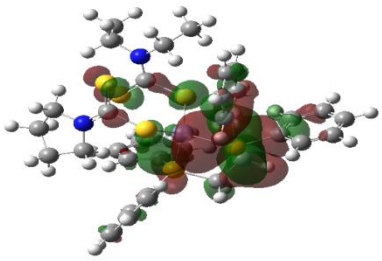
HOMO	LUMO
5	
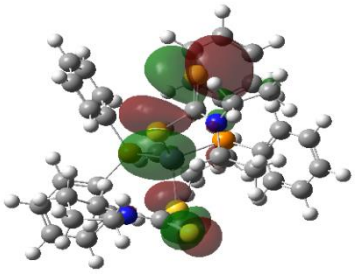	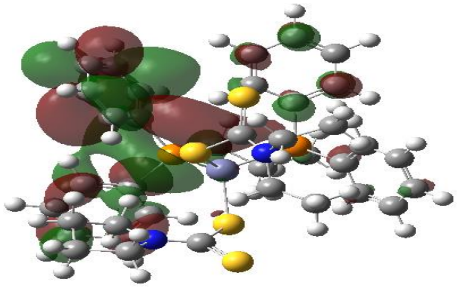
HOMO	LUMO
6	

Figure 2- HOMO-LUMO molecular orbitals of the complexes 1, 2, 5 and 6.